arXiv:cond-mat/0109190v1 [cond-mat.stat-mech] 11 Sep 2001

Exact numerical solution for a time-dependent fiber-bundle model with continuous damage

L. Moral
Departamento de Matemática Aplicada, Universidad de Zaragoza, 50009 Zaragoza, Spain.

J.B. Gómez
Departamento de Ciencias de la Tierra, Universidad de Zaragoza, 50009 Zaragoza, Spain.

Y. Moreno
The Abdus Salam International Centre for Theoretical Physics, Condensed Matter Group, P.O. Box 586, Trieste, I-34014, Italy.

A.F. Pacheco
Departamento de Física Teórica, Universidad de Zaragoza, 50009 Zaragoza, Spain.
(February 1, 2008)

A time-dependent global fiber-bundle model of fracture with continuous damage was recently formulated in terms of an autonomous differential system and numerically solved by applying a discrete probabilistic method. In this paper we provide a method to obtain the exact numerical solution for this problem. It is based on the introduction of successive integrating parameters which permits a robust inversion of the numerical integrations appearing in the problem.

PACS number(s): 46.50.+a, 62.20.Fe, 62.20.Mk.

I. INTRODUCTION

Fracture in disordered media has for many years attracted much scientific and industrial interest [1–7]. An important class of models of material failure is the fiber-bundle models (FBM) which have been extensively studied during the past decades [7–12]. These models consist of a set of parallel fibers having statistically distributed strengths. The sample is loaded parallel to the fiber direction, and a fiber fails if the load acting on it exceeds a strength threshold value. When a fiber fails, its load is transferred to other surviving fibers in the bundle, according to a specific transfer rule. Among the possible options of load transfer, one simplification that makes the problem analytically tractable is the assumption of equal load sharing (ELS), or global load transfer, which means that after each fiber breaks, its stress is equally distributed among the intact fibers. Until very recently, the failure rule applied in standard FBM was discontinuous and irreversible, i.e., when the local load exceeds the failure threshold of a fiber, the fiber is removed from the calculation and is never restored. Recently, a novel continuous damage law was incorporated into these models [13,14]. Thus, when the strength threshold of a fiber is exceeded, it yields, and the elastic modulus of the fiber is reduced by a factor a ($0 < a < 1$). Multiple yields of a given fiber are allowed, up to a maximum of n yielding events per fiber, where n is a small integer number which can be different for each fiber. This generalization of the standard FBM is suitable to describe a variety of elasto-plastic constitutive behaviors [15–17].

The standard FBMs simulate the failure of a system at the *microscopic* level. Each fiber breakage can be mapped onto a new microcrack (with a typical size of a few μm), or onto the extension of a previous microcrack. On the other hand, the continuous damage FBMs simulate failure at a *mesoscopic* level. Now, each fiber in the model can be viewed as a small volume of the material. The term "small" depends on the size of the heterogeneities, but can be of the order of one millimeter for rocks. In each of these representative elementary volumes (REVs) in which the total volume can be divided, there are many potential sites for crack nucleation and growth, and the addition of each new crack will change continuously the elastic properties of the REV until its final failure when the accumulated damage surpasses a threshold. This threshold is identified in our model with the parameter n. Another important parameter in the model, the stiffness reduction factor, a, controls the amount of weakening that each yielding event introduces in a REV. The value $a = 1$ means no weakening, so that the elastic modulus of the REV remains the same irrespective of the number of yieldings, a rather unphysical situation. At the other extreme, the value $a = 0$ means complete weakening after the first yield event. Thus, $0 < a < 1$ is the physically meaningful range for the stiffness reduction factor. In all the results given in the following sections, we have assumed that the initial elastic module of all the REVs is unity and that n is the same for all the fibers. The

randomness is incorporated in the REVs' liftimes, not in the elastic moduli.

FBMs come in two settings, static and time-dependent or dynamic, and both of them have been applied to the standard and continuous damage settings [13,14,18,19]. The static version of FBM simulates the failure of materials by quasistatic loading. Drawing an analogy with what is carried out in a deformation experiment in the laboratory, a static FBM simulates a uniaxial or triaxial, compressive or tensile, deformation test where the duration of the test is measured in seconds or minutes. In these models, the stress on each fiber is the independent variable and the strength of each element is the distributed random variable. On the other hand, the dynamic FBM simulates failure by creep rupture, static fatigue, or delayed rupture, i.e., a (usually) constant load is imposed on the system and the elements break because of fatigue after a period of time. The time elapsed until the system collapses is the lifetime of the bundle. Time acts as an independent variable, and the initial lifetime of each element, for a prescribed initial stress, is the independent identically distributed random quantity. Again, we can draw a clear analogy with a particular type of deformation experiments in the laboratory, the so-called creep experiments, where a heterogeneous material (rock, concrete, composite, ceramic alloy) is subjected to a constant or cyclic load, breaking after a period of time. The duration of these tests depends on the load imposed on the material and, more exactly, on the load compared to the short-term strength of the material (*i.e.*, the load that causes the "instantaneous" failure of the same material in a fast uniaxial experiment). This load is usually expressed as a percentage of the short-term strength and the duration of the experiments is critically dependent on it. For rock, say, a sample will fail by creep after a few hours when subjected to a load 80% of the short-term strength, after a few weeks for a load 70% of the short-term strength, and after a few months or even years for lower working loads. The mechanism behind creep failure is *subcritical crack growth*, *i.e.*, the slow extension of microcracks with lengths smaller than the critical crack length for instantaneous failure. Subcritical crack growth is due to a variety of processes operating near crack tips, the most important of them being *stress corrosion*, a chemical interaction between the crack tip and the environmental species, notably water, filling the microcracks that provokes the hydrolytic weakening of the atomic bonds of the material in the crack tip, where stress concentrations are highest. The crack propagation velocity is extremely sensitive to the applied load, suggesting exponential or power-law velocity functions with large coefficients or exponents.

Indeed, in the dynamic FBMs the most widely used breaking rate function is the power law [10–12], in which elements break at a rate proportional to a power of their stress, σ^ρ, where the exponent ρ is an integer called the stress corrosion exponent, for obvious reasons. This type of breaking rate will be assumed here and is another parameter of the model.

Our generalization of the dynamic global FBM [18] was restricted to the global transfer modality, and there we assumed that the size of the bundle, N, was very large. This enabled us to formulate the evolution of the system in terms of continuous differential equations. This type of equation, similar to those appearing in radioactivity, was first used by Coleman [8], and later in [11]. In [18] we supposed an ELS bundle formed by N fibers which breaks because of stress corrosion under the action of an external constant load $F = N \cdot \sigma_0$, with $\sigma_0 = 1$. The breaking rate of the fibers, Γ, is assumed to be of the power-law type, $\Gamma = \sigma^\rho$, f denotes the strain of the bundle and $Y = 1$ represents the initial stiffness of the individual fibers. The original dynamic FBM was generalized by allowing one fiber to fail more than once, and thus we define the integer n as the maximum value of failures allowed per fiber. Besides, as mentioned before, the parameter a (< 1) represents the factor of reduction in the stiffness of the fibers when they fail. As up to n partial yielding events are permitted per fiber, at any one time the population of fibers will be sorted in $n + 2$ lists. Thus $N = N_0 + N_1 + \ldots + N_n + N'$, where N_i ($i = 0, \ldots, n$) denotes the number of elements that have failed i times. N' denotes the number of elements that have failed $n + 1$ times and therefore are inactive (i.e., they no longer support any load anymore). At $t = 0$, the N elements of the bundle form the list 0, $N_0 = N$, and at $t = T$, $N' = N$. The specification, at a given time t, of the value of N_i, for $i = 0, 1, \ldots, n$, provides the state of the system. In our continuous formulation the N_i are real positive numbers lower than N.

As the external load $F = N$ is supported by the present active fibers, we have $N = f \cdot (N_0 + aN_1 + a^2N_2 + \ldots + a^nN_n)$, and hence

$$f = N/(N_0 + aN_1 + a^2N_2 + \ldots + a^nN_n). \tag{1.1}$$

The time evolution equations are [18]:

$$\begin{aligned}
\frac{dN_0}{dt} &= f^\rho(-N_0),\\
\frac{dN_1}{dt} &= f^\rho(N_0 - \kappa N_1),\\
\frac{dN_2}{dt} &= f^\rho\kappa(N_1 - \kappa N_2),\\
&\vdots \qquad\qquad \vdots\\
\frac{dN_n}{dt} &= f^\rho\kappa^{n-1}(N_{n-1} - \kappa N_n),
\end{aligned} \tag{1.2}$$

where the ubiquitous constant factor κ represents $\kappa = a^\rho$. This is an autonomous differential system. Its solution must fulfill the initial condition

$$\begin{aligned}
N_0(t = 0) &= N\\
N_j(t = 0) &= 0, \quad j \neq 0.
\end{aligned} \tag{1.3}$$

An alternative way of introducing a time-dependent rheological response in FBM is that of Cruz-Hidalgo *et.*

al. [19]. These authors incorporate a viscoelastic constitutive behaviour in their model through the mapping of each fiber to a Kelvin-Voigt element. They express the time evolution of the strain in *each* fiber by way of a differential equation. In their model, fibers break irreversibly when they surpass a statistically distributed strain threshold, whereas in our model multiple failures (yields) of a fiber are allowed, the variable which is statistically distributed is the lifetime of the fibers, and there is no explicit threshold dynamics. This different formulation implies that we can formulate the evolution of the system in terms of coupled differential equations, while the authors in ref. [19] have necessarily to use Monte Carlo simulations due to the lack of a global differential equation for the system.

In reference [18], Eqs. (1.2) were solved by applying a numerical probabilistic method. The purpose of this paper is to present an exact numerical method that solves Eq. (1.2), fulfilling the initial conditions (1.3). This method is explained in Section II. In Section III we present a discussion of the method and of the results. The reader will find a longer discussion of the physical results in Ref. [18]. This paper concentrates on the solution method.

II. EXACT NUMERICAL METHOD

To simplify the notation, we first normalize the variables

$$x_i = \frac{N_i}{N}, \quad i = 0, 1, \cdots, n. \tag{2.1}$$

In terms of the x_i, the differential system to be solved is

$$\begin{aligned} \dot{x}_0 &= -f^\rho x_0 \\ \dot{x}_j &= f^\rho \kappa^{j-1}(x_{j-1} - \kappa x_j) \\ x_0(0) = 1, &\quad x_j(0) = 0, \quad j = 1, 2, \cdots, n. \end{aligned} \tag{2.2}$$

A dot on a variable means derivation with respect to time, and f and κ are the same objects as in Section I:

$$1/f = \sum_{i=0}^{n} a^i x_i. \tag{2.3}$$

The system (2.2) admits a reduction of degrees of freedom by eliminating t from the last n equations and by integrating with respect to x_0:

$$\begin{aligned} \dot{x}_0 &= -f^\rho x_0, \\ \frac{dx_j}{dx_0} &= \frac{\kappa^{j-1}(\kappa x_j - x_{j-1})}{x_0}. \end{aligned} \tag{2.4}$$

From Eq. (2.4) we obtain

$$x_j = \sum_{l=0}^{i} b_l^{(i)} x_0^{\kappa^l}, \quad i = 0, 1, \cdots, n, \tag{2.5}$$

with

$$\begin{aligned} b_0^{(0)} &= 1 \\ b_l^{(j)} &= \frac{b_l^{(j-1)} \kappa^{(j-1)}}{\kappa^j - \kappa^l} \\ b_j^{(j)} &= -\sum_{l=0}^{j-1} b_l^{(j)}, \quad j = 1, 2, \cdots, n. \end{aligned} \tag{2.6}$$

In consequence,

$$\begin{aligned} f &= \frac{1}{\sum_{i=0}^{n} a^i x_i} = \frac{1}{\sum_{i=0}^{n} \alpha_i x_0^{\kappa^i}} =: f_0(x_0) \\ \alpha_i &= \sum_{l=i}^{n} a^l b_l^i. \end{aligned} \tag{2.7}$$

Then, the first equation in (2.4) provides the relation x_0 versus t

$$t = \int_{x_0}^{1} \frac{dx_0}{[f_0(x_0)]^\rho \, x_0} = \int_{x_0}^{1} \frac{\left(\sum_{i=0}^{n} \alpha_i x_0^{\kappa^i}\right)^\rho}{x_0} dx_0 \tag{2.8}$$

which, in principle, solves the problem because it relates t to x_0 and hence to any other x_j. However, the integral (2.8) is, in general, improper for $x_0 \to 0$ because the integrand is $O(x_0^{\rho\kappa^n - 1})$ and therefore the numerical relation t vs. x_0 is problematic. Specifically:

a) If $\rho\kappa^n - 1 \leq 0$ this integral is proper,

b) if $\rho\kappa^n - 1 > 0$ the integral is improper.

Due to the fact that the convergence occurs iff $\rho\kappa^n - 1 > -1$, Eq. (2.8) is always convergent, because in our model of fracture $\rho\kappa^n > 0$.

Let $\epsilon \in (0, 1)$; due to the fact that x_0 decays from 1 to 0, there exists a time value $t_0 > 0$ such that $x_0(t_0) = \epsilon$. If (2.8) is improper, we perform the following change of parameter: $x_0 \equiv y_0 \to y_1$, such that

$$\begin{aligned} \dot{x}_0 &= -f^\rho x_0 \\ \dot{y}_1 &= -\kappa f^\rho y_1 \\ \dot{x}_j &= f^\rho \kappa^{j-1} \left[x_{j-1} - \kappa x_j\right]; \quad j = 1, 2, \cdots, n, \end{aligned} \tag{2.9}$$

with $x_0(t_0) = \epsilon$, $y_1(t_0) = 1$, and $t > t_0$. From here

$$\frac{dx_0}{dy_1} = \frac{\kappa x_0}{y_1} \Rightarrow x_0 = c_1 y_1^{1/\kappa}, \quad c_1 = (x_0(t_0)) = \epsilon. \tag{2.10}$$

Hence

$$x_j = \sum_{l=0}^{j} b_l^{(j)} \left(\epsilon y_1^{1/\kappa}\right)^{\kappa^l} = \sum_{l=0}^{j} \beta_l^{(j,1)} y_1^{\kappa^{l-1}}, \tag{2.11}$$

$$f =: f_1(y_1) = \frac{1}{\sum_{i=0}^{n} \alpha_i \sum_{l=0}^{i} \beta_l^{(i,1)} y_1^{\kappa^{l-1}}} = \frac{1}{\sum_{i=0}^{n} \alpha_i^{(1)} y_1^{\kappa^{i-1}}} \tag{2.12}$$

with $\beta_l^{(i,1)} = b_l^{(i)}\epsilon^{\kappa^l}$, $\alpha_i^{(1)} = \sum_{l=i}^n \alpha_l \beta_i^{(i,1)}$ $(i = 0, 1, \cdots, n)$.

In these circumstances (2.11) and the equation

$$t - t_0 = \int_{y_1}^1 \frac{dy_1}{(f_1(y_1))^\rho\, y_1} = \int_{y_1}^1 \frac{\left(\sum_{i=0}^n \alpha_i^{(1)} y_1^{\kappa^{i-1}}\right)^\rho}{y_1} dy_1 \tag{2.13}$$

describe t, $x_0, \cdots, x_n$ in terms of the y_1 parameter, for $t \geq t_0$.

As the integrand of (2.13) is $O(y_1^{\rho\kappa^{n-1}-1})$, then

a) If $\rho\kappa^{n-1} - 1 \geq 0$ (2.13) is a proper integral,

b) if $\rho\kappa^{n-1} - 1 < 0$ (2.13) is an improper integral, but (2.13) is always convergent.

Now, as y_1 decays to zero, there exists a time instant $t_1 > t_0$ such that $y_1(t_1) = \epsilon$. And by considering the change of parameter $y_1 \to y_2$ given by the conditions

$$\begin{aligned} \dot{x}_0 &= -f^\rho x_0 \\ \dot{y}_1 &= -\kappa f^\rho y_1 \\ \dot{y}_2 &= -\kappa^2 f^\rho y_2 \\ \dot{x}_j &= f^\rho \kappa^{j-1} \left[x_{j-1} - \kappa x_j\right]; \quad j = 1, 2, \cdots, n, \end{aligned} \tag{2.14}$$

with $y_2(t_2) = \epsilon$, $y_2(t_1) = 1$, and $t > t_1$, we have

$$\frac{dy_1}{dy_2} = \frac{\kappa y_1}{y_2} \Rightarrow y_1 = c_2 y_2^{1/\kappa}, \quad c_2 = (y_1(t_1)) = \epsilon, \tag{2.15}$$

and hence

$$x_j = \sum_{l=0}^j b_l^{(j,1)} \left(\epsilon y_2^{1/\kappa}\right)^{\kappa^{l-1}} = \sum_{l=0}^j \beta_l^{(j,2)} y_2^{\kappa^{l-2}}, \tag{2.16}$$

$$f =: f_2(y_2) = \frac{1}{\sum_{i=0}^n \alpha_i^{(2)} y_2^{\kappa^{i-2}}} \tag{2.17}$$

with identical meaning as before for $\beta_l^{(j,2)}$ and $\alpha_j^{(2)}$. Then, (2.16) and

$$t - t_1 = \int_{y_2}^1 \frac{dy_2}{(f_2(y_2))^\rho\, y_2} = \int_{y_2}^1 \frac{\left(\sum_{i=0}^n \alpha_i^{(2)} y_2^{\kappa^{i-2}}\right)^\rho}{y_2} dy_2 \tag{2.18}$$

describe t, $x_0, \cdots, x_n$ in terms of y_2, for $t \geq t_1$. Besides, as the integrand of (2.18) is $O(y_2^{\rho\kappa^{n-2}-1})$, then

a) if $\rho\kappa^{n-2} - 1 \geq 0$ (2.18) is a proper integral,

b) if $\rho\kappa^{n-2} - 1 < 0$ (2.18) is an improper integral, but always convergent.

The process followed so far is generalized in the way expressed in Table I where in the end

$$f =: f_n(y_n) = \frac{1}{\sum_{i=0}^n \alpha_i^{(n)} y_n^{\kappa^{i-n}}}, \tag{2.19}$$

and therefore

$$t - t_{n-1} = \int_{y_n}^1 \frac{dy_n}{(f_n(y_n))^\rho\, y_n} = \int_{y_n}^1 \frac{\left(\sum_{i=0}^n \alpha_i^{(n)} y_n^{\kappa^{i-n}}\right)^\rho}{y_n} dy_n, \tag{2.20}$$

whose integrand is $O(y_n^{\rho-1})$, that is, integral (2.20) is always proper.

III. RESULTS AND CONCLUSIONS

The simple formalism written in Section II can be expressed, for example, in a brief program of MATHEMATICA and its results graphically appreciated. We omit here the program but it can be provided on request. By fixing the constants at the following values: $n = 3$, $a = 0.6$, $\rho = 2$, and $\epsilon = 0.1$, in Fig. 1 the value of the working parameters y_i are represented vs. time. Note that their range of definition is from 1 to ϵ, except for y_3 which ends at 0 for $t_3 = T$, i.e., the actual lifetime of the bundle.

In Fig. 2 we again show the evolution of the working parameters and also the evolution of the four lists x_i of elements in the problem.

The strategy developed in Section II can be summarized in a few sentences. First, let us observe Fig. 2 to appreciate the time evolution of the different lists: while x_0 monotonously declines from 1 at $t = 0$ to 0 at $t = T$, the lists x_j, $j = 1, 2, 3$ start from 0 at $t = 0$, rise to a maximum and then monotonously decline to 0 at $t = T$ (strictly speaking, all the lists vanish at the same time). The last list $j = n$ is special in the sense that it is the only one that tends to 0 with an infinite slope when t tends to T.

The analytical resolution of Eq. (2.2) is impossible because of the nonlinearity introduced by the f^ρ factors. This source of complexity is partly overcome after having recognized the partial reduction of degrees of freedom expressed in (2.4). This partial reduction leads to the relation between x_j, $j = 1, 2, \cdots, n$ and x_0, hence from (2.8) one has solved in principle the time evolution of x_0, and of the rest of x_j. But, in (2.8) one also recognizes that this integral is improper. This is the *real problem* we face for the numerical inversion $t \leftrightarrow x_0$ in the region where x_0 is very small. In intuitive terms, this shows in Fig. 2 because beyond a certain time, x_0 is no longer significant and its relation with t becomes "delicate". Therefore we have used $x_0 = y_0$ as a good integration parameter only up to $t = t_0$. Beyond this point we successively introduced other "artificial parameters" $y_1, y_2, \cdots, y_n$ which in the corresponding time interval play the role performed by x_0 from 0 to t_0. Using these parameters, we are able to robustly relate all the variables x_i to t in the whole interval from 0 to T.

At the end of the process, the last integral is always proper, which allows a robust numerical inversion in the

vicinity of $t = T$. Intuitively, this is clear in Fig. 2 where we appreciate the abrupt fall-off of x_3.

In the comments written in Section II after Eqs. (2.8), (2.13), (2.18), and (2.20) regarding the nature of those integrands, we noted that in general they behave as $O(y_i^{\rho\kappa^{n-i}-1})$. This implies that the condition

$$\rho\kappa^{n-i} - 1 \geq 0 \tag{3.1}$$

tells us the value of $i = i_c$,

$$i_c \geq n - \frac{\ln \rho}{|\ln \kappa|}, \tag{3.2}$$

such that, for $i \geq i_c$, the respective integral is proper and there is no need to introduce more artificial integrating parameters.

The reader should note that the ϵ introduced in the method is not a limiting factor of precision, but merely sets the temporal ranges of the various integrating parameters y_i. In our procedure, the only source of inaccuracy is the precision of MATHEMATICA, used for the numerical inversion of the integrals.

As a final conclusion we would say that the exact numerical method presented in this paper to solve this fiber-bundle problem does not predict any new qualitative result with respect to what was obtained using the approximate method of Ref. [18]. Therefore, no new physical conclusions can be drawn from here.

The use of this exact strategy in other scientific problems that are cast as an autonomous differential system will be considered in the next future. In this respect, clear candidates are some ecological problems and models of infection spreading [20,21].

ACKNOWLEDGMENTS

This work was supported in part by the Spanish DGICYT Project PB98-1594.

[1] *Statistical Models for the Fracture of Disordered Media*. Editors, H.J. Herrman and S. Roux, North Holland (1990), and references therein.

[2] *Statistical Physics of Fracture and Breakdown in Disordered Systems*. B. K. Chakrabarti, L. G. Benguigui, Clarendon Press, Oxford (1997), and references therein.

[3] A. Garcimartin, A. Guarino, L. Bellon, S. Ciliberto, *Phys. Rev. Lett.* **79**, 3202 (1997).

[4] C. Maes, A. van Moffaert, H. Frederix, H. Strauven, *Phys. Rev. B* **57**, 4987 (1998).

[5] A. Petri, G. Paparo, A. Vespignani, A. Alippi, M. Constantini, *Phys. Rev. Lett.* **73**, 3423 (1994).

[6] S. Zapperi, P. Ray, H. E. Stanley, A. Vespignani, *Phys. Rev. Lett.* **78**, 1408 (1997).

[7] Y. Moreno, J. B. Gomez, A. F. Pacheco,*Phys. Rev. Lett.* **85**, 2865 (2000).

[8] B.D. Coleman, *J. Appl. Phys.* **28**, 1058 (1957); *ibid* **28**, 1065 (1957).

[9] S.L. Phoenix and L. Tierney, *Eng. Frature Mech.* **18**, 193 (1983).

[10] W.I. Newman, A.M. Gabrielov, T.A. Durand, S.L. Phoenix and D.L. Turcotte, *Physica D***77**, 200 (1994).

[11] W.I. Newman, D.L. Turcotte and A.M. Gabrielov, *Phys. Rev. E* **52**, 4827 (1995).

[12] M. Vázquez-Prada,J. B. Gómez, Y. Moreno, A. F. Pacheco, *Phys. Rev. E* **60**, 2581 (1999).

[13] S. Zapperi, A. Vespignani, and H. E. Stanley, Nature **388**, 658 (1997).

[14] F. Kun, S. Zapperi, H. J. Herrmann, *Eur. Phys. J.* **B17**, 269 (2000).

[15] A. E. Naaman, H. W. Reinhardt, *High performance fiber reinforced cement composites* (E and FN Spon, London, 1995).

[16] A. G. Evans, J. M. Domergue, E. Vagaggini, *J. Am. Ceramic Soc.* **77**, 1425 (1994).

[17] T. Kanada, V. C. Li, *J. Eng. Mech.* **125**, 290 (1999).

[18] L. Moral, Y. Moreno, J.B. Gómez, and A.F. Pacheco, *Phys. Rev. E*, **63**, (2001).

[19] R. Cruz-Hidalgo, F. Kun, and H. Herrmann, *cond-mat/0103232*, 10 Mar 2001.

[20] M. Rama Mohana Rao, *Ordinary Differential Equations: Theory and Applications*, Edward Arnold Pub. (1981).

[21] B.M. Anderson and R.M. May, *Infection diseases in humans*, Oxford Univ. Press, Oxford (1992).

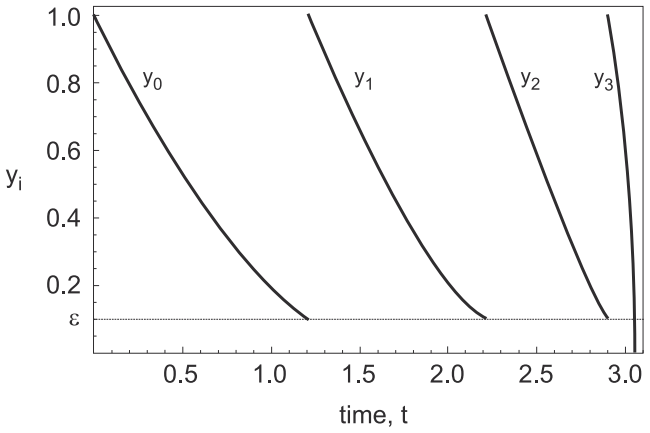

FIG. 1. Time evolution of the four integrating parameters y_0, y_1, y_2 and y_3 for a system with $n = 3$, $a = 0.6$ and $\rho = 2$. Note that their range of definition is from 1 to ϵ, except for y_3, which goes from 1 to 0.

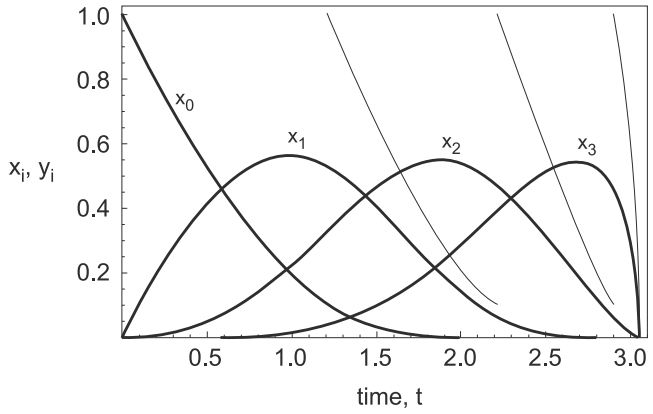

FIG. 2. Time evolution for the four integrating parameters and the four variables x_0, x_1, x_2 and x_3 for a system with the same parameters as for Fig. 1.

TABLE I. General terms in the procedure.

Time interval	Condition	Parameter
$[0, t_0]$		$y_0 = x_0$
$[t_0, t_1]$	$y_0(t_0) = \epsilon$	y_1 such that $\dot{y}_1 = -\kappa f^\rho y_1$; $y_1(t_0) = 1$
$[t_1, t_2]$	$y_1(t_1) = \epsilon$	y_2 such that $\dot{y}_2 = -\kappa^2 f^\rho y_2$; $y_2(t_1) = 1$
$\vdots$	$\vdots$	$\vdots$
$[t_{n-1}, t_n]$	$y_{n-1}(t_{n-1}) = \epsilon$	y_n such that $\dot{y}_n = -\kappa^n f^\rho y_n$; $y_n(t_{n-1}) = 1$